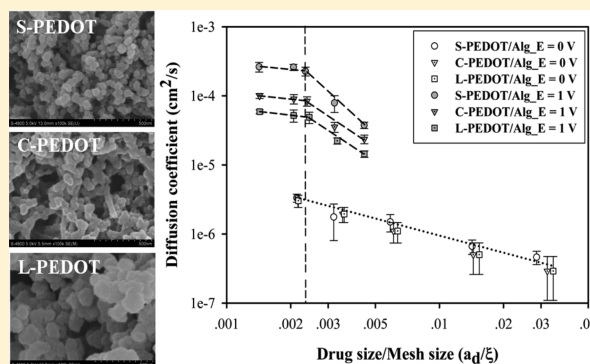


# Electrically Controlled Release of Benzoic Acid from Poly(3,4-ethylenedioxythiophene)/Alginate Matrix: Effect of Conductive Poly(3,4-ethylenedioxythiophene) Morphology

Nophawan Paradee and Anuvat Sirivat\*

Conductivity and Electroactive Polymer Research Unit, The Petroleum and Petrochemical College, Chulalongkorn University, Bangkok 10330, Thailand

**ABSTRACT:** A drug-loaded conductive polymer/hydrogel blend, benzoic acid-loaded poly(3,4-ethylenedioxythiophene/alginate (BA-loaded PEDOT/Alg) hydrogel, was used as a carrier/matrix for an electrical stimuli transdermal drug delivery system (TDDS). The effects of cross-linking ratio, PEDOT particle size, and electric field strength on the release mechanism and the diffusion coefficient ( $D$ ) of BA were examined by using a modified Franz-diffusion cell. The diffusion scaling exponent value of BA is close to 0.5 which refers to the diffusion controlled mechanism, or the Fickian diffusion as the BA release mechanism. The  $D$  increased when there was a decrease in the cross-linking ratio due to the mesh size-hindering effect. When increasing electric field strength, the  $D$  of BA-loaded PEDOT/Alg hydrogel increased because the cathode-BA<sup>-</sup> electro-repulsion, electroinduced alginate expansion, and PEDOT electroneutralization simultaneously occurred. The highest  $D$  belonged to a blend with the smallest PEDOT particle and highest electrical conductivity. The  $D$  of BA was a function of the matrix mesh size except when drug size/mesh size was lower than  $2.38 \times 10^{-3}$ , where  $D$  of BA became mesh size independent as the matrix mesh size was extremely large. Thus, the fabricated conductive polymer hydrogel blends have a great potential to be used in TDDS under electrical stimulation.



## INTRODUCTION

Transdermal drug delivery system (TDDS) is a route for transporting drugs through the skin and into the circulatory system. There are many advantages for using TDDS such as by passing the first pass metabolism, decreasing in concentrations of drug in blood, decreasing side effects, as well as reducing fluctuations of drug in blood. However, the delivery of drugs via the skin is restricted due to lipophilic nature of skin and molecular drug size.<sup>1–6</sup> Iontophoresis is one of the methods used to enhance drug penetration across the skin by applying an electrical potential. This is especially true for both ionized and un-ionized drugs, including high molecular weight such as peptides, proteins, and oligonucleotides.<sup>4–6</sup>

Hydrogel is one class of polymer-based controlled drug release matrices. The physical and chemical cross-linking process can produce a hydrophilic polymer as hydrogel by converting the soluble polymer chains into an insoluble polymer networks.<sup>7,8</sup> Besides exhibiting swelling behavior in water, other environmental conditions may still affect hydrogel volume change: temperature, pH, ionic concentration, solvent composition, and external electrical stimuli.<sup>9,10</sup> However, hydrogel is not an excellent material for response under electrical stimuli due to the relatively low electrical conductivity of the polymer matrix.<sup>11</sup>

Stimulus-responsive hydrogels or smart hydrogels can potentially be used for the development of controlled drug

release under applied electric field because the change in the structure of the polymer can change the drug release ability in response to the electrical potential. Electrochemically controlled drug release, using a conductive polymer, has been used in drug release systems.<sup>12</sup> A conducting polymer is composed of a conjugated polymer chain, which can promote  $\pi$ -electron delocalizing along the polymer backbone and contributes to electrical conductivity. Conductive polymers combined with drugs are prepared with ease on conductive substrates to form various patterns and shapes, and drug release is precisely controlled under applied electrical current or potential stimuli.<sup>12</sup> Ge et al.<sup>13</sup> prepared a stimuli-responsive material for electrical drug delivery. Poly[(D,L-lactic acid)-co-(glycolic acid)]-*b*-poly(ethylene oxide)-*b*-poly[D,L-lactic acid]-co-(glycolic acid)] was used as the hydrogel matrix combined with polypyrrole (PPy) nanoparticles loaded with fluorescein or daunorubicin as the model drugs. The chemical synthesis produced negatively charged fluorescein or positively charged daunorubicin incorporated into the PPy nanoparticles. The drugs in PPy nanoparticles were able to prevent the unwanted release from the hydrogel without an applied electric field. Under applied electric field, the fluorescein was released upon

Received: December 24, 2013

Revised: June 19, 2014

Published: July 16, 2014

reduction, while the oxidation reaction could promote the release of daunorubicin. The amount of drug released increased with increasing electrical potential.<sup>13</sup>

In this work, poly(3,4-ethylenedioxythiophene) (PEDOT) was selected as the conductive polymer for a drug substrate and blended with a hydrogel because of high conductivity in the doped state.<sup>14</sup> Alginate (Alg), which has biocompatibility, nontoxicity, and transparency, was used as the hydrogel matrix.<sup>15</sup> The objective of this work was to study the release mechanism of a combined conductive polymer/hydrogel system as PEDOT/alginate (PEDOT/Alg) hydrogel for controlled release of benzoic acid under applied electric field. The release profile and release kinetics of benzoic acid from blend films were investigated based on the effects of the matrix mesh size, PEDOT particle size, and electric field strength.

## EXPERIMENTAL SECTION

**Materials.** Alginic acid sodium salt (Na-Alg) from brown algae, 3,4-ethylenedioxythiophene (EDOT), benzoic acid (BA), and 2-(*N*-morpholino) ethanesulfonic acid (MES) monohydrate were purchased from Sigma-Aldrich to act as a matrix, monomer, model drug, and buffer solution, respectively. Calcium chloride dihydrate ( $\text{CaCl}_2 \cdot \text{H}_2\text{O}$ ) was used as a cross-linking agent and purchased from Ajax Finechem. Ammonium peroxydisulfate (APS) was purchased from Qrec and used as an oxidizing initiator. Acetone, methanol, and dimethyl sulfoxide (DMSO) were purchased from Labscan.

**Synthesis of Benzoic Acid-Loaded Poly(3,4-ethylenedioxythiophene) (BA-Loaded PEDOT).** BA-loaded PEDOT was prepared by dropping EDOT monomers into a solution that consisted of APS and BA dissolved in distilled water, then it was stirred for 72 h. The preparation of PEDOT particles without BA was similar to the preparation of BA-loaded PEDOT except that the solution before doping EDOT monomer only consisted of APS. The color of solution transformed from yellow to green, then blue to dark blue during that time. The product was separated from the solution by using centrifugal separation and washed with methanol and acetone solution (methanol:acetone = 20:3). Lastly, the product was dried in a vacuum oven at 60 °C for 24 h. The BA-loaded PEDOT particles, at various doping levels (molar of EDOT:molar of APS), were synthesized by various amounts of APS as noted in Table 1.

**Table 1. Condition of Synthesis BA-Loaded PEDOT at 0.15 M of EDOT and 0.45 M of BA**

doping level (molar of EDOT: molar of APS)	APS (M)
1:1	0.15
1:2	0.30
1:3	0.45

**Preparation of Benzoic Acid-Loaded Poly(3,4-ethylenedioxythiophene)/Alginate Hydrogel (BA-Loaded PEDOT/Alg).** Na-Alg solution with 0.4% w/v was prepared by dissolving Na-Alg powder in distilled water. Then BA-loaded PEDOT powder (25 mg) was added to the Na-Alg solution under constant stirring. In order to cross-link,  $\text{CaCl}_2$  was added to the solution under constant stirring at various cross-linking ratios (moles of cross-linking agent/mol of uronic acid monomer unit): 0.3, 0.5, 0.7, 1.0, and 1.3. Each solution was cast onto a mold and dried at 40 °C for 72 h to obtain the

homogeneous BA-loaded PEDOT/Alg hydrogel films of various cross-linking ratios with a film thickness of  $\sim 0.3$  mm.<sup>16</sup>

**BA-Loaded PEDOT Characterization.** The functional groups of the BA-loaded PEDOT particle were identified using a Fourier-transform infrared spectroscopy (FTIR; Thermo Nicolet, Nexus670). The spectrometer was set up in absorption mode using KBr as the background material with 64 scans, a resolution of  $\pm 4$   $\text{cm}^{-1}$ , and covering the wavenumber range of 400–4000  $\text{cm}^{-1}$ .

The thermal behavior of BA-loaded PEDOT particles was examined using a thermogravimetric analyzer (TGA; PerkinElmer, TGA7). An aluminum pan was loaded with samples (5–10 mg). The change of mass was investigated under nitrogen atmosphere from 30 to 900 °C at a heating rate of 10 °C/min.

The morphology of BA-loaded PEDOT was studied using a scanning electron microscopy (SEM; Hitachi, S4800) which was operated in an acceleration voltage of 5 kV and a magnification of 100 k.

Electrical conductivity of the BA-loaded PEDOT was measured by using a custom-built two-point probe connected with an electrometer (Keithley, Model 6517A), which supplied the voltage and recorded the current. The Van der Pauw method was used to estimate the current to find the linear Ohmic regime. The linear Ohmic regime, which consisted of applied voltage and resultant current, was transformed to the electrical conductivity of BA-loaded PEDOT using eq 1:

$$\sigma = \frac{1}{\rho} = \frac{1}{R_s \times t} = \frac{I}{K \times V \times t} \quad (1)$$

where  $\sigma$  is the specific conductivity (S/cm),  $\rho$  is the specific resistivity ( $\Omega$  cm),  $R_s$  is the sheet resistivity ( $\Omega$ ),  $I$  is the measured current (A),  $K$  is the geometric correction factor ( $3.53 \times 10^{-3}$ ),  $V$  is the applied voltage (V), and  $t$  is the pellet thickness (cm).

**PEDOT/Alginate Hydrogel (PEDOT/Alg Hydrogel) Characterization.** The molecular weight between cross-links ( $\bar{M}_c$ ) and the mesh size ( $\xi$ ) correlates to the release behavior of the drug and the physical properties of hydrogel were determined. A hydrogel sample was immersed in MES buffer solution (pH 5.5) after it was weighed in air and heptane. After the hydrogel sample was swollen to equilibrium for 5 day, it was weighed in air and heptanes again. Lastly, the sample was dried at 40 °C in vacuum oven for 5 days, then weighed in air and heptanes one more time. Various weights were used to determine the polymer volume fraction.<sup>17</sup>

The  $\bar{M}_c$  was calculated by the Flory–Rehner equation as follows in eq 2:<sup>17,18</sup>

$$\frac{1}{\bar{M}_c} = \frac{2}{\bar{M}_n} - \frac{\left(\frac{\bar{v}}{V_1}\right) [\ln(1 - v_{2,s}) + v_{2,s} + \chi_1(v_{2,s})^2]}{v_{2,r} [(v_{2,s}/v_{2,r})^{1/3} - 0.5(v_{2,s}/v_{2,r})]} \quad (2)$$

where  $\bar{M}_n$  is the number-averaged molecular weight of the polymer before cross-linking ( $\bar{M}_n = 450\,000$  g/mol),  $\bar{v}$  is the specific volume of Alg ( $\bar{v} = 0.60$   $\text{cm}^3/\text{g}$  of Alg),<sup>18</sup>  $V_1$  is the molar volume of the water ( $V_1 = 18$   $\text{mol}/\text{cm}^3$ ),<sup>18</sup>  $v_{2,r}$  is the volume fraction of the polymer in a relaxed state,  $v_{2,s}$  is the volume fraction of the polymer in a swollen state, and the Flory polymer–solvent interaction parameter ( $\chi_1$ ) for Alg is 0.473.<sup>18</sup>

The  $\xi$  was determined using eq 3:<sup>19,20</sup>

$$\xi = v_{2,s}^{-1/3} \left[ C_n \left( \frac{2\bar{M}_c}{M_r} \right) \right]^{1/2} l \quad (3)$$

where  $C_n$  is the Flory characteristic ratio ( $C_n = 27.33$ ),<sup>19</sup>  $l$  is the carbon–carbon bond length of the monomer unit ( $l = 5.15$  Å),<sup>20</sup>  $M_r$  is monomer molecular weight ( $M_r = 198$  g/mol),<sup>20</sup> and  $\bar{M}_c$  is the molecular weight between cross-links.

**Preparation of MES Buffer pH 5.5.** A MES buffer solution was selected to simulate human skin. MES solution 0.1 M (at pH 5.5) was prepared and poured into the receptor chamber of a modified Franz-Diffusion cell.

**Spectrophotometric Analysis of Drug.** The maximum absorption wavelength of BA was investigated using a UV/Visible spectrophotometer (UV-TECAN infinite M200). The absorbance value at the peak wavelength of BA corresponded to the BA concentration, thus BA calibration curves were created.

**Actual Drug Content.** The actual amount of BA in the BA-loaded PEDOT was determined by dissolving the BA-loaded PEDOT (0.6 g) in 4 mL of DMSO. Next, the solution (0.5 mL) of BA-loaded PEDOT in DMSO was added to the MES buffer solution (0.8 mL). The amount of BA in the solution was determined by the UV/Visible spectrum peaks (at the wavelengths of 232 nm), which were associated with the calibration curves in order to determine the actual drug content.

**Drug Release Studies.** Modified Franz-diffusion cells were used to study the diffusion of BA from BA-loaded PEDOT/Alg hydrogels as shown in Figure 1. A diffusion cell is composed of

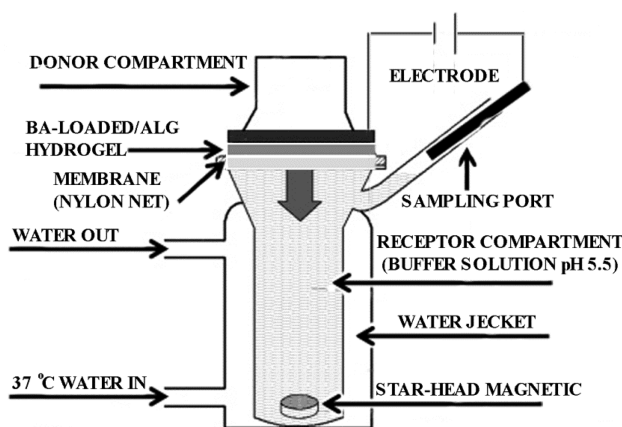


Figure 1. Modified Franz-Diffusion cell experiment set up.

two component chambers as receptor and donor chambers. The receptor chamber was filled with MES buffer solution (pH 5.5) and kept at  $37 \pm 2$  °C via a circulating water bath. The donor component was exposed to ambient conditions. The BA-loaded PEDOT/Alg hydrogel sample was placed over a nylon net (mesh size =  $2.25 \text{ mm}^2$ ), which was on top of the receptor chamber. The area available for BA diffusion was  $2.51 \text{ cm}^2$ . The MES buffer solution was stirred throughout the experiment for 48 h and came into contact in the receptor chamber. An electric field (various electrical voltages of 0, 0.01, 0.05, 0.5, 0.8, and 1.0 V) was applied on the surface of the hydrogel, nylon net, and buffer solution via an aluminum cathode electrode that was connected to a power supply (KEITHLEY 1100 V Source Meter). The diffusion of BA occurred when it passed through the polymer matrix and nylon net into the solution. A sample (0.1 mL) was taken out at specific times and replaced with fresh

buffer solution at an equal volume. The drug amount was determined by a UV/Visible spectrophotometer.<sup>16</sup>

**Release Characteristics of BA from BA-Loaded PEDOT/Alg Hydrogel.** The release mechanism of BA was studied by the Korsmeyer–Peppas model, as shown in eq 4,<sup>21,22</sup> which explains the drug release from the polymeric system. The amount of drug released was fitted with the Korsmeyer–Peppas model,<sup>21,22</sup> a power law in time:

$$\frac{M_t}{M_\infty} = kt^n \quad (4)$$

where  $M_t/M_\infty$  is the fraction of the drug released at time  $t$ ,  $k$  is the kinetic constant (unit of  $T^{-n}$ ), and  $n$  is the diffusion scaling exponent for drug release, which is used to characterize different release mechanisms. Furthermore, Higuchi's equation as shown in eq 5<sup>22,23</sup> indicates the fraction of drug release from the matrix and is proportional to the square root of time.

$$\frac{M_t}{M_\infty} = k_H t^{1/2} \quad (5)$$

where  $M_t$  and  $M_\infty$  are the masses of drug released at the times equal to  $t$  and infinite time, respectively, and  $k_H$  is the Higuchi constant (unit of  $T^{-n}$ ). The Higuchi equation corresponds to a particular case of eq 4 when  $n$  is precisely equal to 0.5. If the Higuchi drug release (i.e., Fickian diffusion) is obeyed, then a plot of  $M_t/M_\infty$  versus  $t^{1/2}$  will be a straight line with a slope of  $k_H$ .

The diffusion coefficient of the BA from the PEDOT/Alg hydrogels was calculated from a slope of plot between drug accumulation and the square root of time according to the Higuchi equation as in eq 6:<sup>23,24</sup>

$$M_t = 2C_0 A \left( \frac{Dt}{\pi} \right)^{1/2} \quad (6)$$

where  $M_t$  is the amount of drug released (g),  $A$  is the diffusion area ( $\text{cm}^2$ ),  $C_0$  is the initial drug concentration in the hydrogel ( $\text{g}/\text{cm}^3$ ), and  $D$  is the diffusion coefficient of the drug ( $\text{cm}^2/\text{s}$ ).

## RESULTS AND DISCUSSION

**BA-loaded PEDOT Characterization.** Figure 2a shows the FTIR spectra of BA, PEDOT, and BA-loaded PEDOT. The peaks of BA at 2835 and  $1700 \text{ cm}^{-1}$  can be referred to as the O–H and C=O bonds. The benzene ring peak appears at  $900\text{--}1000 \text{ cm}^{-1}$ .<sup>25</sup> For the PEDOT particle synthesized without BA, stretching of quinoidal structure in the thiophene ring and stretching of the thiophene ring are presented as peaks at 1519 and  $1356 \text{ cm}^{-1}$ , which originated from the C–C or C=C respectively. The peaks at 1206 and  $1098 \text{ cm}^{-1}$  refer to the stretching vibration of the C–O–C bond in the EDOT. The peaks at 980, 843, and  $700 \text{ cm}^{-1}$  can be referred to as the C–S bond in the thiophene ring.<sup>26,27</sup> The absorption peaks of BA-loaded PEDOT are similar to those of PEDOT except a peak at  $1682 \text{ cm}^{-1}$  appears, which indicates benzoate anion loaded PEDOT. This peak is referred to as the carboxylate group ( $\text{COO}^-$ ) of BA, which interacts with PEDOT. Furthermore, the thermal stability of BA-loaded PEDOT was examined using TGA. The thermogram is shown in Figure 2b. The decomposition temperature of BA showed up at 135 °C. The PEDOT showed a decomposition temperature of 210 °C as the dopant degradation of  $\text{SO}_4^{2-}$  from APS, and in the region between 310 to 420 °C the polymer backbone degradation occurred.<sup>28</sup> The decomposition temperature of



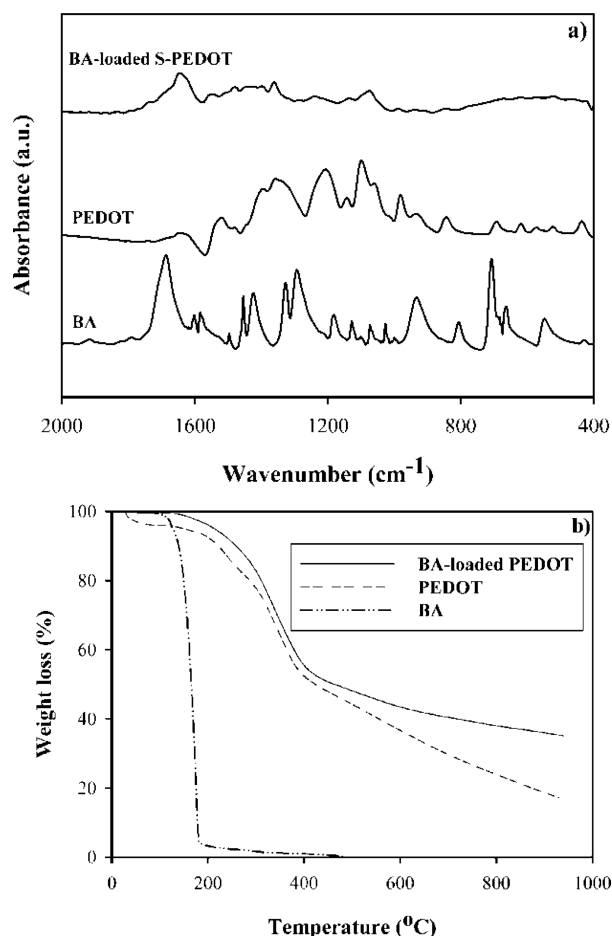


**Figure 2.** (a) Absorption infrared spectra and (b) thermogravimetric thermograms of BA, PEDOT, and BA-loaded PEDOT.

BA-loaded PEDOT shifted to 215 °C for the dopant and 320–460 for the polymer backbone. Furthermore, the observed changes in thermal stability were accompanied by increasing char residue, showing that existing BA with PEDOT as BA-loaded PEDOT offered higher thermal resistance. This resulted from the electrostatic interaction between the carboxylate group of BA and the positively charged PEDOT sites as shown by FTIR at 1682 cm<sup>-1</sup>.<sup>29,30</sup>

The BA-loaded PEDOT nanoparticles at various APS concentrations show various particle sizes and shapes, as shown in Figure 3. The particle sizes of BA-loaded PEDOT are 220 nm irregular shape (L-PEDOT), 71 nm raspberry agglomerate shape (S-PEDOT), and 108 nm coralliform shape (C-PEDOT). They were synthesized by 0.15, 0.30, and 0.45 M of APS concentrations, respectively. The BA-loaded PEDOT particle sizes and shapes vary a great deal with APS concentration, in which it acted as an oxidizing initiator affecting the rate of polymerization and PEDOT polymeric cation amount as shown in Figure 4. In the first step, EDOT is

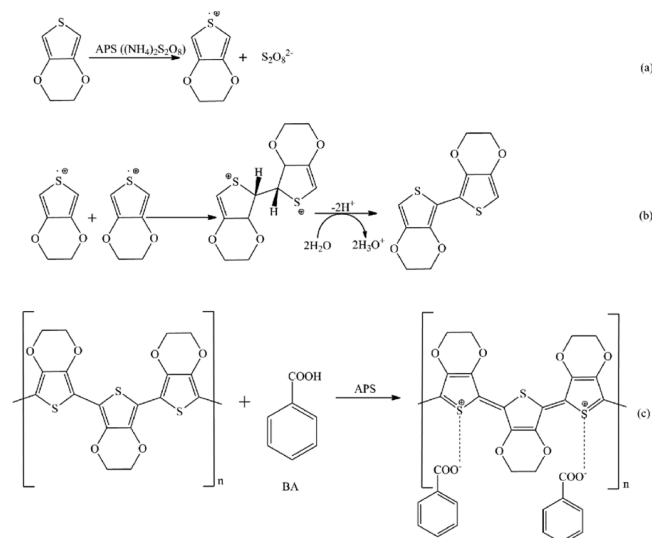


**Figure 4.** Proposed polymerization mechanism of BA-loaded PEDOT: (a) EDOT as a monomer is oxidized by APS to a cation radical; (b) EDOT cation radicals form dimers that subsequently are deprotonated; and (c) PEDOT polymer is doped by benzoate ion.

oxidized by APS to become EDOT cation radical, which forms EDOT dimers via protonation and deprotonation, respectively. The process is duplicated to polymerize and to obtain PEDOT. Finally, the polymerized PEDOT is doped by the counterions as the benzoate ions.<sup>26,31</sup> The structure was confirmed by FTIR and TGA (Figures 2a,b).

A greater amount of PEDOT polymeric cations is due to a higher APS concentration creating a stronger electrorepulsive

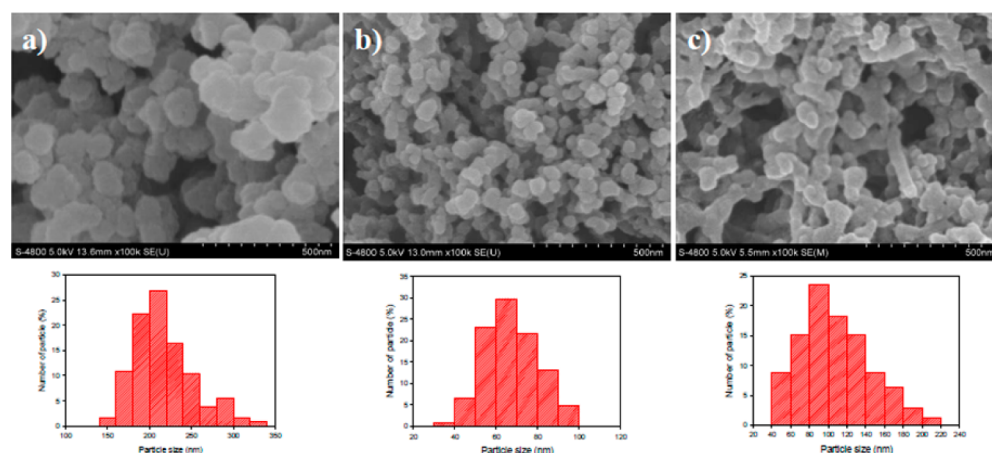


**Figure 3.** Morphologies and size distributions of BA-loaded PEDOT at various APS concentrations: (a) 0.15 M, (b) 0.30 M, and (c) 0.45 M.

force between PEDOT polymeric cation radicals, leading to a smaller particle size. On the other hand, a higher APS concentration ( $>0.3$  M) enhances the sulfate counteranions of APS, which generates the screening effect of the electro-repulsive reaction. This is the cause of the agglomeration of PEDOT particles resulting in a larger particle size as the coralliform shape.<sup>26</sup>

Table 2 shows the relationship between electrical conductivity and BA-loaded PEDOT particle size. The electrical

**Table 2. Particle Size and Electrical Conductivity of BA-Loaded PEDOT and Actual Amount of Benzoic Acid in PEDOT**

drug-loaded PEDOT	particle size (nm)	electrical conductivity (S/cm)
BA-loaded S-PEDOT	$71 \pm 43$	$95.64 \pm 5.52$
BA-loaded C-PEDOT	$108 \pm 43$	$10.65 \pm 3.86$
BA-loaded L-PEDOT	$220 \pm 37$	$2.78 \pm 4.35$

conductivity values are 95.64, 10.65, and 2.78 S/cm for BA loaded S-PEDOT, C-PEDOT, and L-PEDOT, respectively. Electrical conductivity increases as the particle size decreases because the smaller particle size has a higher surface area for electron to transfer, and thus higher electrical conductivity.<sup>26,27</sup> Moreover, the electrical conductivity of BA-loaded-C-PEDOT is lower than that of BA-loaded-S-PEDOT because the coralliform shape is a result from PEDOT particles aggregation which possesses a lower surface area and greater free space for electron to transfer, thus reducing electron mobility.<sup>26</sup>

**PEDOT/Alg Hydrogel Characterization.** The PEDOT/Alg hydrogels were prepared at various cross-linking ratios (0.3, 0.5, 0.7, 1.0, and 1.3) and various PEDOT particle sizes and shapes (S-PEDOT, C-PEDOT, and L-PEDOT). The  $\bar{M}_c$  and  $\xi$  of the PEDOT/Alg hydrogels were investigated to characterize the porous structure of the hydrogels with and without applied electric field. The  $\bar{M}_c$  and  $\xi$  are larger at a lower cross-linking ratio because there is a longer Alg strand between cross-links and easier more relaxed swelling behavior, which is produced via a lower cross-linker resulting in larger  $\bar{M}_c$  and  $\xi$ .<sup>16</sup> The  $\bar{M}_c$  and  $\xi$  without electric field decrease when PEDOT particles are added to the Alg hydrogel in the preparation of the PEDOT/Alg hydrogel because the PEDOT/Alg hydrogel is more rigid than the Alg hydrogel due to the existing PEDOT particles restricting chain movement and relaxation; thus, the PEDOT/Alg hydrogel exhibits less swelling, and a smaller mesh size results.<sup>32,33</sup> The  $\xi$  of the Alg hydrogel varies between 641 and 3313 Å at an electric field strength of 0 V and between 1277 and 3887 Å at an electric field strength of 1 V as shown in Figure 5. The  $\xi$  of PEDOT/Alg hydrogel varies between 171 and 2626 Å at an electric field strength of 0 V and between 1282 and 3930 Å at an electric field strength of 1 V. Thus,  $\xi$  under applied electric field is larger than that with no electric field applied. The electric field affects Alg chain expansion through the resultant electrorepulsive force between the negatively charged electrode and negatively charged carboxylate group in the Alg structure, so-called “electroinduced Alg expansion”.<sup>16</sup> The  $\xi$  of the PEDOT/Alg hydrogel increases with decreasing PEDOT particle size, due to more free volume for water adsorption.

**Release Characteristics of BA from BA-Loaded PEDOT/Alg Hydrogel.** In order to study the release mechanism of BA from the BA-loaded PEDOT/Alg hydrogel, the actual amount of BA within the hydrogel sample was

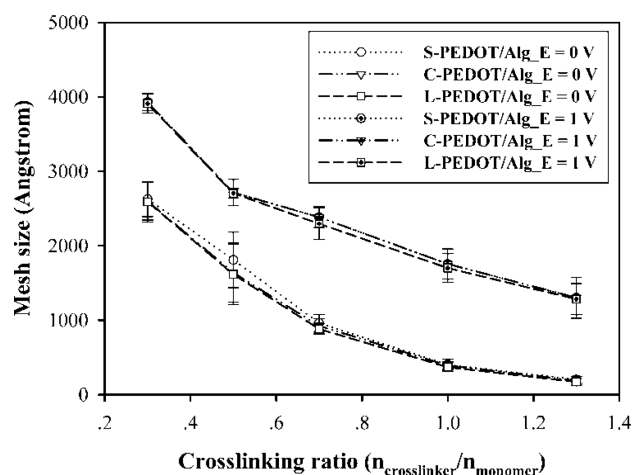


**Figure 5.** Mesh size of PEDOT/Alg hydrogel at various cross-linking ratios under electric field strength of 0 and 1 V.

determined as a percentage of the BA amount presents relative to the amount actually loaded in the BA-loaded PEDOT/Alg samples. The actual amounts of BA in the samples were  $95.4 \pm 5.1$ ,  $93.8 \pm 7.8$ , and  $94.1 \pm 6.3\%$  for the BA-loaded S-PEDOT, C-PEDOT, and L-PEDOT/Alg hydrogels, respectively.

**Effect of Electric Field Strength.** The release mechanism of BA from the BA-loaded PEDOT/Alg hydrogel was analyzed using the diffusion scaling exponent ( $n$ ) from eq 4. The  $n$  value is the slope of the curve of the plot between  $\log(M_t/M_\infty)$  and  $\log$  time, (Figure 6). The  $n$  values of the BA-loaded PEDOT/

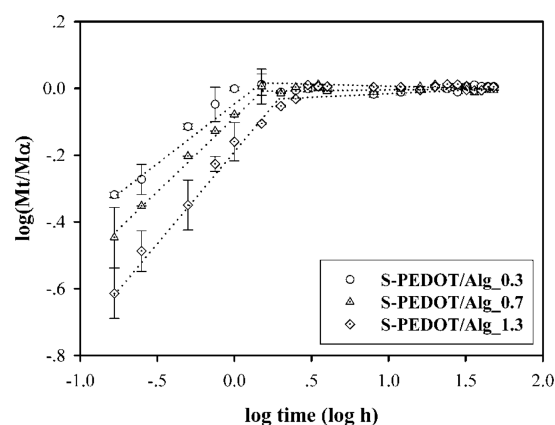


**Figure 6.** Plot of  $\log M_t/M_\infty$  versus  $\log$  time of benzoic acid released from variously cross-linked S-PEDOT/Alg hydrogels at electric field strength of 1 V.

Alg hydrogels are tabulated in Tables 3 and 4 at electric field strengths of 0 and 1 V, respectively. The  $n$  values are between 0.41 and 0.58, which are quite close to 0.5 in both cases, thus the release of BA is the diffusion controlled mechanism or the Fickian diffusion.<sup>22</sup> The PEDOT/Alg hydrogels act as a diffusion barrier, and BA is released mainly by the diffusion mechanism as supported by the swelling behavior.<sup>34,35</sup>

The amount of BA released from the BA-loaded PEDOT/Alg hydrogel increases steadily up to 1 h after that it approaches equilibrium. Plotting the release of BA as a function of the square root of time shows a linear relationship in the first 1 h. In Figure 7a, with the absence of an electric field, the BA molecules are gradually released from the BA-loaded S-PEDOT/Alg hydrogel until the amount of BA released reaches

Table 3. Release Kinetic Parameters and the Linear Regression Values Obtained from Fitting the Drug Release Experimental Data

cross-linking ratio of Ca-Alg	release kinetics								
	S-PEDOT			C-PEDOT			L-PEDOT		
	$n$	$k_H(h^{-n})$	$r^2$	$n$	$k_H(h^{-n})$	$r^2$	$n$	$k_H(h^{-n})$	$r^2$
0.3	0.49	0.98	0.9834	0.47	1.09	0.9756	0.48	0.9912	0.9943
0.5	0.48	0.92	0.9922	0.45	1.07	0.9876	0.46	0.9874	0.9874
0.7	0.44	0.86	0.9833	0.42	1.06	0.9833	0.42	0.9718	0.9611
1.0	0.42	0.84	0.9785	0.41	0.98	0.9678	0.41	0.9585	0.9802
1.3	0.42	0.78	0.9876	0.41	0.96	0.9832	0.41	0.9412	0.9798

Table 4. Release Kinetic Parameters and the Linear Regression Values Obtained from Fitting the Drug Release Experimental Data at an Electric Field Strength of 1 V

cross-linking ratio of Ca-Alg	release kinetics								
	S-PEDOT			C-PEDOT			L-PEDOT		
	$n$	$k_H(h^{-n})$	$r^2$	$n$	$k_H(h^{-n})$	$r^2$	$n$	$k_H(h^{-n})$	$r^2$
0.3	0.58	1.00	0.9689	0.59	1.06	0.9698	0.52	0.99	0.9716
0.5	0.56	0.96	0.9461	0.58	1.05	0.9682	0.52	0.98	0.9653
0.7	0.55	0.92	0.9708	0.56	1.02	0.9669	0.52	0.97	0.9527
1.0	0.54	0.88	0.9833	0.55	0.92	0.9947	0.51	0.95	0.9761
1.3	0.50	0.75	0.9288	0.54	0.85	0.9499	0.50	0.82	0.9689

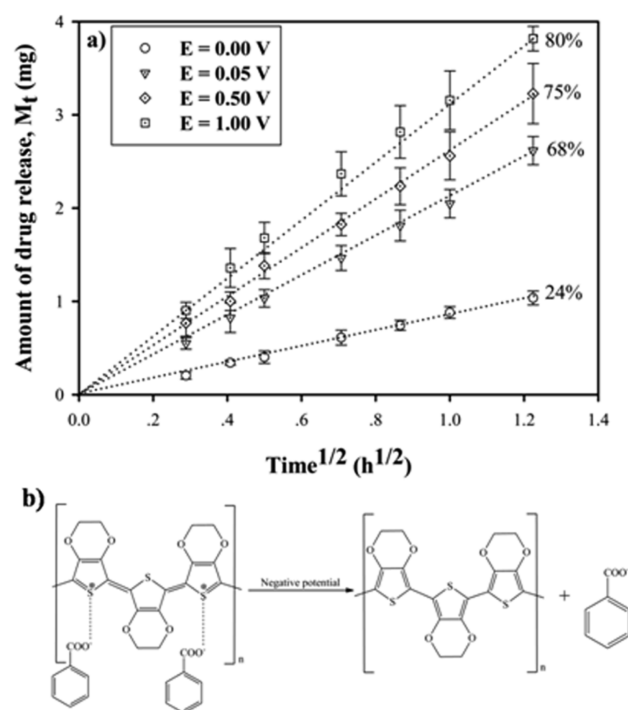


Figure 7. (a) Amount of benzoic acid released from S-PEDOT/Alg\_0.7 hydrogels at various electric field strengths. (b) Release reaction of benzoic acid from BA-loaded PEDOT/Alg hydrogel under applied electric field.

equilibrium. Moreover, the amount of BA released from the BA-loaded S-PEDOT/Alg hydrogel is higher with an increase in electric field strength (cathode in a donor part represents a negatively charged electrode). The electric field generates the driving force to enhance the BA diffusion from the electro-repulsive force between the negatively charged BA and the negatively charged electrode, so-called “cathode–BA<sup>−</sup> electro-repulsion”, as shown in Figure 4b.<sup>36–38</sup> In addition, the electric field also creates electroinduced Alg expansion, which produces

the expansion of hydrogel matrix, a larger mesh size, and a corresponding increase in the BA diffusion.<sup>16</sup> Lastly, the electric field strength enhances the release of BA as it provides a stronger reduction reaction of the BA-loaded S-PEDOT as shown in Figure 7b. The PEDOT chain in the reduced form is produced and contracted via electron injection under electric field, this causes squeezing BA<sup>−</sup> out of neutralized PEDOT with lesser electrostatic binding interaction, inducing higher drug release, so-called “PEDOT electroneutralization”.<sup>36,39</sup>

The  $D$  of each system was calculated from the slope of the Higuchi's equation, which is the plot between  $M_t$  and  $t^{1/2}$ . Figure 8 shows the  $D$  of BA increases with increasing electric

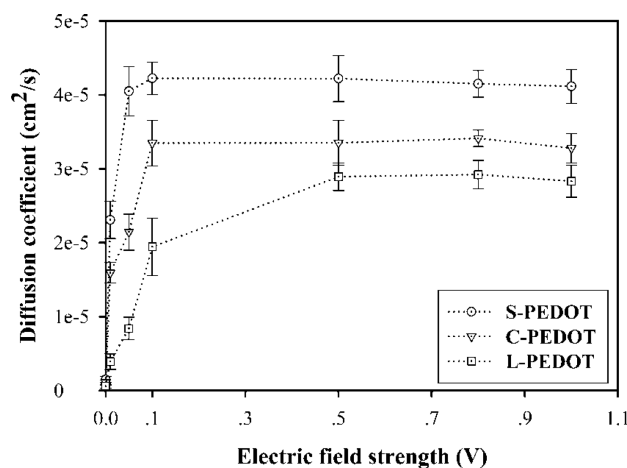


Figure 8. Diffusion coefficient of benzoic acid from PEDOT/Alg\_0.7 of various PEDOT particle sizes versus electric field strength.

field strength ( $E = 0$ –1 V at the current of 0–0.25  $\mu\text{A}$ ) under cathode as an electrode (negative charge) in the donor part. Increasing electric field strength produces greater cathode–BA<sup>−</sup> electrorepulsion, facilitating the diffusion of BA from the polymer matrix.<sup>16,40</sup> Furthermore, the particle size of PEDOT affects the  $D$  of BA under applied electric field. The  $D$  at a given

applied electric field strength of BA-loaded S-PEDOT has the highest value, followed by the BA-loaded C-PEDOT, and the BA-loaded L-PEDOT, respectively. The smaller PEDOT particle size exhibits higher electrical conductivity than the larger particle size; this induces electron to transfer more easily as an electric field is applied. Safranin dye was studied for its release characteristics under applied electric field ( $E = -0.1$  V) from a semi-interpenetrating polyaniline-polyacrylamide (PANI-PAAM) network by Lira and Torresi.<sup>41</sup> The safranin release under electric field was greater than without an electric field because the reduced PANI chains created more free volume within the hydrogel, therefore, safranin diffusion increased.<sup>41</sup> Furthermore, heparin was investigated for release from polypyrrole-poly(vinyl alcohol) with applied electric field ( $E = 1$  mA) by Li et al.<sup>42</sup> The amount of heparin released was greater than with no applied electric field. There were several factors in which electric field controls releasing: charged drug electrophoresis reactions, drug doped conductive polymer reduction reactions, mesh size expansion, and increased or decreased pH due to  $H^+$  migration toward the cathode.<sup>42</sup>

**Effect of Cross-Linking Ratio.** The amount of BA released decreases with increasing cross-linking ratio (as shown in Figure 6) because smaller mesh size at a higher cross-linking ratio results in a smaller pathway for BA to diffuse, the so-called "mesh size-hindering effect".<sup>16</sup>

In Figure 9, the cross-linking ratio and mesh size at the electric field strengths of 0 and 1 V affect the  $D$  of BA from the

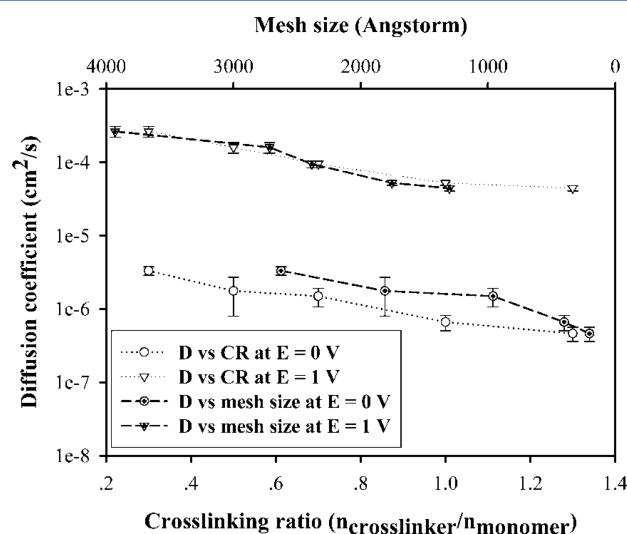


**Figure 9.** Diffusion coefficient of benzoic acid from S-PEDOT/Alg as a function of cross-linking ratio and mesh size at electric field strength of 0 and 1 V.

BA-loaded S-PEDOT/Alg hydrogels. The  $D$  of BA decreases with increasing cross-linking ratio because the mesh size-hindering effect retards BA diffusion. In addition, the  $D$  of BA under electric field is higher than that without electric field because the cathode-BA<sup>-</sup> electrorepulsion, electroinduced Alg expansion, and PEDOT electroneutralization are created as an electric field is applied.<sup>16,36–40</sup>

**Effect of Electrode Polarity.** The amount of BA release and the  $D$  under cathode are greater than that of no applied electric field, and under anode (positive charge) as electrode in the donor part, as shown in Figure 10. Thus, the electric field under cathode placed on hydrogel generates the cathode-BA<sup>-</sup>

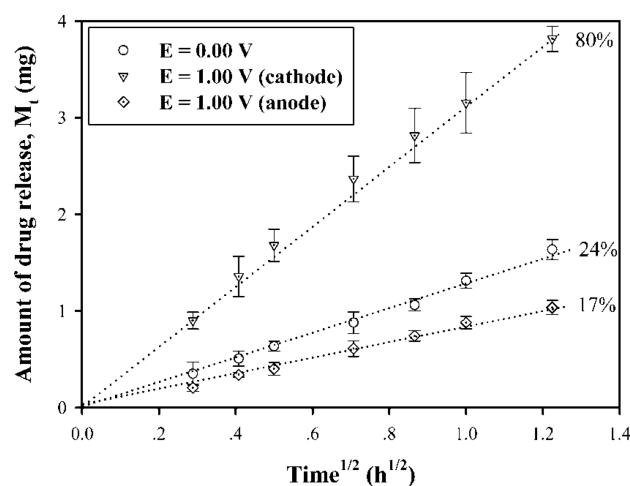


**Figure 10.** Amounts of benzoic acid released from S-PEDOT/Alg\_0.7 hydrogels at electric field strengths of 0 and 1 V with hydrogel samples attached to anode or cathode.

electrorepulsion, which enhances BA diffusion from the BA-loaded PEDOT/Alg hydrogel. On the other hand, the diffusion of BA is retarded when the anode electrode is placed on the hydrogel because it creates an electroattractive force between the positively charged electrode and the negatively charged BA resulting in restricted BA diffusion.<sup>16,40</sup>

The log-log plot of the  $D$  as a function of the ratio of drug size over mesh size of hydrogel under the electric field strengths of 0 and 1 V at 37 °C is shown in Figure 11. The scaling exponent,  $m$ , can be determined from eq 7:

$$D = D_0(a_d/\xi)^{-m} \quad (7)$$

where  $D$  is the diffusion coefficient of the drug;  $D_0$  is the diffusion coefficient at a very small drug size;  $a_d$  is the drug size (5.58 Å);  $\xi$  is the apparent mesh size of the hydrogel, and  $m$  is the scaling exponent.<sup>16,40</sup>

The  $m$  values for the BA diffusion through the Alg matrix and the PEDOT/Alg matrix without electric field are 1.06<sup>16</sup> and 1.95, respectively, and the  $D_0$  values are  $2.01 \times 10^{-716}$  and  $1.02 \times 10^{-9}$  cm<sup>2</sup>/s, respectively. The  $m$  values under applied electric field ( $E = 1$  V) of Alg, S-PEDOT/Alg, C-PEDOT/Alg, and the L-PEDOT/Alg hydrogel are 1.28,<sup>16</sup> 1.13, 1.05, and 1.31, respectively and the  $D_0$  values are  $2.08 \times 10^{-6}$ ,<sup>16</sup>  $1.89 \times 10^{-9}$ ,  $1.97 \times 10^{-8}$ ,  $6.57 \times 10^{-9}$  cm<sup>2</sup>/s, respectively.

Figure 11a,b shows decreasing diffusion when  $a_d/\xi$  increases due to the mesh size-hindering effect. In all cases of applied electric field (cathode in the donor part), the  $D$  can be divided onto two regimes, when  $a_d/\xi$  is below and above  $2.38 \times 10^{-3}$ . Below  $2.38 \times 10^{-3}$ , the diffusion is  $a_d/\xi$  independent because this  $a_d/\xi$  range also provides easy drug penetration. Above  $2.38 \times 10^{-3}$ ,  $D$  decreases monotonically.

Furthermore, Figure 12 shows the comparison of the values of the drug from the Alg, S-PEDOT/Alg, C-PEDOT/Alg, L-PEDOT/Alg, and the polypyrrole/poly(acrylic acid) (PPy/PAA) hydrogels at various conditions. The higher  $D$  values of the drugs under these conditions are due to lower cross-linking ratios and smaller drug sizes. In addition, the  $D$  increases under applied electric field due to cathode-BA<sup>-</sup> electrorepulsion, a larger mesh size, inducing easier drug mobility through the hydrogels. Nevertheless, the  $D$  of BA from the Alg hydrogel is higher than that of the BA-loaded PEDOT/Alg hydrogel without electric field because the free volume or pathway for



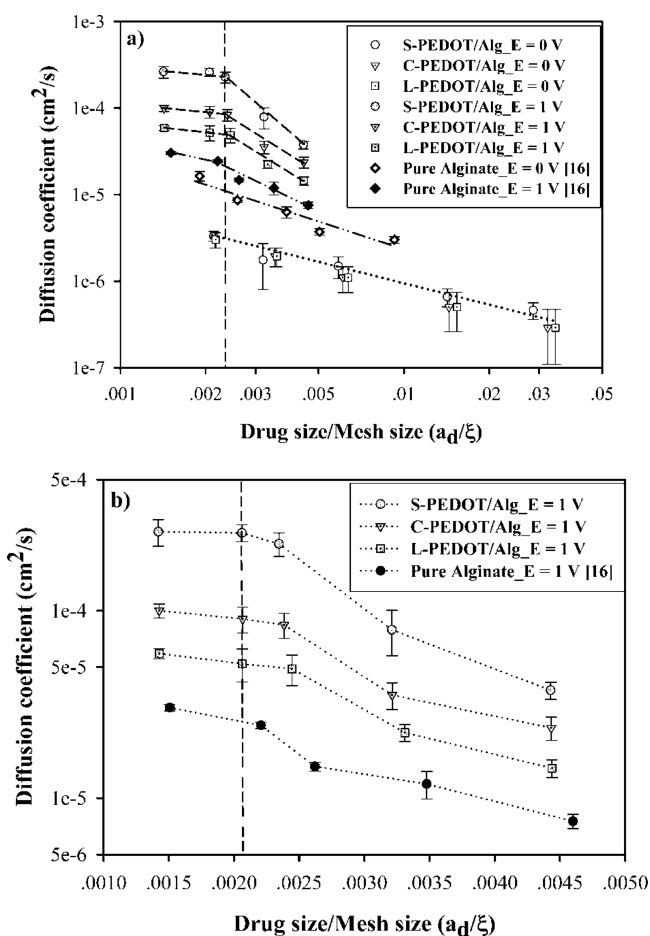


**Figure 11.** Diffusion coefficient of (a) benzoic acid from alginate and PEDOT/Alg hydrogel at electric field strengths of 0 and 1 V and (b) benzoic acid from PEDOT/Alg hydrogel at electric field strength of 1 V.

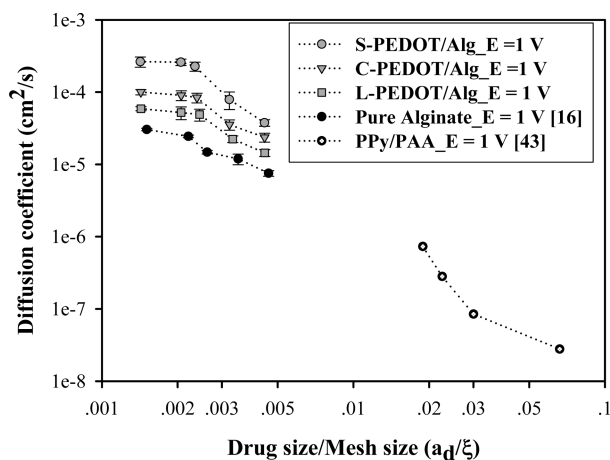


**Figure 12.** Diffusion coefficient of drug from alginate, PEDOT/Alg, and PPy/PAA hydrogel at electric field strength of 1 V.

drug diffusion is reduced by the presence of PEDOT particles. In addition, the  $D$  under applied electric field of the BA-loaded PEDOT is higher than that of BA-loaded Alg hydrogel. The  $D$  of the BA-loaded S-PEDOT/Alg hydrogel is the highest because it has the greatest electrical conductivity, resulting in easier electron transfer for the reduction reaction of BA-loaded PEDOT. On the other hand, Chansai et al.<sup>43</sup> studied the  $D$  of

sulfosalicylic acid (SSA) from the PPy/PAA hydrogel under electric field.<sup>43</sup> SSA was loaded on the PPy structure by chemical oxidation reaction using ammonium persulfate as an initiator. The PPy/PAA blend film was prepared by dispersing SSA-loaded PPy powder in the acrylic solution and cast on mold to obtain the film. In Figure 12, the  $D$  of BA from the PEDOT/Alg hydrogel is higher than that of SSA diffusion from PPy/PAA hydrogel because of the larger mesh size of PEDOT/Alg hydrogel, greater electrical conductivity of PEDOT (electrical conductivity of SSA-doped PPy = 51.836 S/cm), and a smaller drug size.

Thus, the diffusion of BA and SSA as anionic drugs through the Alg, PEDOT/Alg, and the PPy/PAA hydrogel occur through the concentration gradient under no applied electric field, and by the electrophoresis of negatively charged drugs under applied electric field. The PEDOT/Alg hydrogel in this study is available for TDDS application because many available PEDOT size critically affect specific controlled release conditions, especially under applied electric field. In addition, the presence of PEDOT allows electrical triggering for drug release to exist in the matrix system.

## CONCLUSIONS

Polyethylenedioxythiophene/alginate hydrogel acted as a carrier/matrix for the controlled release of benzoic acid. The release behavior and the diffusion coefficient were studied for the effect of cross-linking ratio, PEDOT particle size, electric field strength, and electrode polarity. The release mechanism of BA was the diffusion controlled mechanism or the Fickian diffusion because the diffusion scaling exponent is close to 0.5. The  $D$  of BA increased with decreasing cross-linking ratio due to the mesh size-hindering effect. When electric field was applied under cathode placed on the hydrogel, the  $D$  was greater than that of no electric field because the electric field induced cathode-BA<sup>-</sup> electrorepulsion, electroinduced Alg expansion, and PEDOT electroneutralization. The  $D$  of BA-loaded S-PEDOT was the greater under applied electric field at the PEDOT particle size was smallest resulting in the highest electrical conductivity. The  $D$  of BA depended on the electrode polarity, under cathode placed on the hydrogel, the  $D$  of BA was higher than that of no electric field and anode placed on the hydrogel because cathode-BA<sup>-</sup> electrorepulsion was generated. Thus, the  $D$  of BA was critically dependent on the mesh size except when the drug size/mesh size was lower than  $2.38 \times 10^{-3}$ ; the mesh size had no effect toward BA diffusion because the matrix provided a too large pathway relative to the drug size. Hence, the fabricated conductive polymer hydrogel blends is potentially applicable in TDDS under electrical stimulation.

## AUTHOR INFORMATION

### Corresponding Author

\*Tel: 662 218 4131, Fax: 662 611 7221, E-mail: anuvat.s@chula.ac.th.

### Notes

The authors declare no competing financial interest.

## ACKNOWLEDGMENTS

The authors would like to acknowledge the financial support provided by the Thailand Research Fund (TRF-RTA, RGJ PHD/0285/2551); the Royal Thai Government; the Conductive and Electroactive Polymer Research Unit; the



Petroleum and Petrochemical College, Chulalongkorn University; and the Ratchadaphiseksomphot Endowment Fund of Chulalongkorn University.

## REFERENCES

- (1) Keleb, E.; Sharma, R. K.; B Mosa, E.; Z Aljahwi, A.-A. *Int. J. Adv. Pharm. Sci.* **2010**, *1*, 201–211.
- (2) Shingade, G. M.; Quazi, A.; Sabale, P. M.; Grampurohit, N. D.; Gadhave, M. V.; Jashav, S. L.; Gaikwad, D. D. *J. Drug Delivery Ther.* **2012**, *2*, 66–75.
- (3) Latheeshjlal, L.; Phanitejaswini, P.; Soujanya, Y.; Swapna, U.; Sarika, V.; Moulika, G. *Int. J. PharmTech Res.* **2011**, *3*, 2140–2148.
- (4) Dixit, N.; Bali, V.; Baboota, S.; Ahuja, A.; Ali, J. *Curr. Drug Delivery* **2007**, *4*, 1–10.
- (5) Zorec, B.; Preat, V.; Miklavcic, D.; Pavselj, N. *Pregledni Clanek* **2013**, *82*, 339–359.
- (6) Khan, A.; Yasir, M.; Asif, M.; Chauhan, I.; Singh, A. P.; Sharma, R.; Singh, P.; Rai, S. *J. Appl. Pharm. Sci.* **2011**, *01*, 11–24.
- (7) Green, R. A.; Baek, S.; Poole-Warren, L. A.; Martens, P. J. *Sci. Technol. Adv. Mater.* **2010**, *11*, 1–13.
- (8) Gupta, P.; Vermani, K.; Grag, S. *Drug Discovery Today* **2002**, *7*, 569–579.
- (9) Kim, S.-J.; Yoon, S.-G.; Lee, S.-M.; Lee, J.-H.; Kim, S. I. *Sens. Actuators, B* **2003**, *96*, 1–5.
- (10) Qiu, Y.; Park, K. *Adv. Drug Deliver. Rev.* **2001**, *53*, 321–339.
- (11) Kim, D.-H.; Abidian, M.; Martin, D. C. *J. Biomed. Mater. Res., Part A* **2004**, *71*, 577–585.
- (12) Luo, X.; Cui, X.-T. *Electrochem. Commun.* **2009**, *11*, 402–404.
- (13) Ge, J.; Neofytou, E.; Cahill, T. J.; Beygui, R. E.; Zare, R. N. *ACS Nano* **2012**, *6*, 227–233.
- (14) Oh, S.-G.; Im, S.-S. *Curr. Appl. Phys.* **2002**, *2*, 273–277.
- (15) Pasparakis, G.; Bouropoulos, N. *Int. J. Pharm.* **2006**, *323*, 34–42.
- (16) Paradee, N.; Sirivat, A.; Niamlang, S.; Prissanaroon-Oujai, W. *J. Mater. Sci.: Mater. Med.* **2012**, *23*, 999–1010.
- (17) Peppas, N. A.; Wright, S. I. *Eur. J. Pharm. Biopharm.* **1998**, *1*, 15–29.
- (18) Wells, L. A.; Sheardown, H. *Eur. J. Pharm. Biopharm.* **2011**, *79*, 304–313.
- (19) Canal, T.; Peppas, N. A. *J. Biomed. Mater. Res.* **1989**, *23*, 1183–1193.
- (20) Chan, A. W.; Neufeld, R. J. *Biomaterials* **2009**, *30*, 6119–6129.
- (21) Korsmeyer, R. W.; Gurny, R.; Doelker, E.; Buri, P.; Peppas, N. A. *Int. J. Pharm.* **1983**, *15*, 25–35.
- (22) Pradhan, R.; Budhathoki, U.; Thapa, P. *Kathmandu Univ. J. Sci., Eng. Technol.* **2008**, *1*, 55–67.
- (23) Higuchi, T. *J. Pharm. Sci.* **1963**, *52*, 1145–1149.
- (24) Reichling, J.; Landvatter, U.; Wagner, H.; Kostka, K.-H.; Schaefer, U. F. *Eur. J. Pharm. Biopharm.* **2006**, *64*, 222–228.
- (25) Hayashi, S.; Kimura, N. *Bull. Inst. Chem. Res., Kyoto Univ.* **1966**, *335*–340.
- (26) Paradee, N.; Sirivat, A. *Polym. Int.* **2014**, *63*, 106–113.
- (27) Yang, Y.; Jiang, Y.; Xu, J.; Yu, J. *Polymer* **2007**, *48*, 4459–4465.
- (28) Choi, J. W.; Han, M. G.; Kim, S. Y.; Oh, S. G.; Im, S. S. *Synthetic Metal* **2004**, *141*, 293–299.
- (29) Xiao-hong, G.; Guang-hao, C.; Chii, S. *J. Environ. Sci.* **2007**, *19*, 438–443.
- (30) Kowalewska, B.; Miecznikowski, K.; Makowski, O.; Palys, B.; Adamczyk, L.; Kulesza, P. *J. Solid State Electrochem.* **2007**, *1023*–1030.
- (31) Mueller, M.; Fabretto, M.; Evans, D.; Hojati-Talemi, P.; Gruber, C.; Murphy, P. *Polymer* **2012**, *53*, 2146–2151.
- (32) Dispenza, C.; Presti, C. L.; Belfiore, C.; Spadaro, G.; Piazza, S. *Polymer* **2006**, *47*, 961–971.
- (33) Hezaveh, H.; Muhamad, I.-I. *Carbohydr. Polym.* **2012**, *89*, 138–145.
- (34) Thakur, A.; Wanchoo, R. K.; Singh, P. *Chem. Biochem. Eng. Q.* **2011**, *25*, 471–482.
- (35) Huang, Y.; Zhang, B.; Xu, G.; Hao, W. *Compos. Sci. Technol.* **2013**, *84*, 15–22.
- (36) Niamlang, S.; Sirivat, A. *Int. J. Pharm.* **2009**, *371*, 126–133.
- (37) Murdan, S. *J. Controlled Release* **2003**, *92*, 1–7.
- (38) Kantaria, S.; Rees, G. D.; Lawrence, M. J. *J. Controlled Release* **1999**, *60*, 355–365.
- (39) Gordon, G. W.; Geoffrey, M. S.; Leon, A.P. K.; Peter, R. T. *Conductive Electroactive Polymers: Intelligent Polymer Systems*, 3rd ed.; CRC Press: Boca Raton, FL, 2009; p 220.
- (40) Juntanon, K.; Niamlang, S.; Rujiravanit, R.; Sirivat, A. *Int. J. Pharm.* **2008**, *356*, 1–11.
- (41) Lira, L. M.; Cordoba de Torresi, S. I. *Electrochem. Commun.* **2005**, *7*, 717–723.
- (42) Li, Y.; Neoh, K. G.; Kang, E. T. *J. Biomed. Mater. Res., Part A* **2005**, *73*, 171–181.
- (43) Chansai, P.; Sirivat, A.; Niamlang, S.; Chotpattananont, D.; Viravaidya-Pasuwat, K. *Int. J. Pharm.* **2009**, *381*, 25–33.